THE JOURNAL OF BIOLOGICAL CHEMISTRY
Vol. 279, No. 18, Issue of April 30, pp. 18323–18333, 2004
Printed in U.S.A.

A Conserved Aspartate (Asp-1393) Regulates NADPH Reduction of Neuronal Nitric-oxide Synthase

IMPLICATIONS FOR CATALYSIS*

Received for publication, September 21, 2003, and in revised form, February 2, 2004
Published, JBC Papers in Press, February 13, 2004, DOI 10.1074/jbc.M310391200

Koustubh Panda‡, Subrata Adak‡§, David Konas, Manisha Sharma, and Dennis J. Stuehr¶

From the Department of Immunology, Lerner Research Institute, The Cleveland Clinic, Cleveland, Ohio 44195

Nitric-oxide synthases (NOSs) are flavo-heme enzymes whose electron transfer reactions are controlled by calmodulin (CaM). The NOS flavoprotein domain includes a ferredoxin-NADP$^+$ reductase (FNR)-like module that contains NADPH- and FAD-binding sites. FNR-like modules in related flavoproteins have three conserved residues that regulate electron transfer between bound NAD(P)H and FAD. To investigate the function of one of these residues in neuronal NOS (nNOS), we generated and characterized mutants that had Val, Glu, or Asn substituted for the conserved Asp-1393. All three mutants exhibited normal composition, spectral properties, and binding of cofactors, substrates, and CaM. All had slower NADPH-dependent cytochrome *c* and ferricyanide reductase activities, which were associated with proportionally slower rates of NADPH-dependent flavin reduction in the CaM-free and CaM-bound states. Rates of NO synthesis were also proportionally slower in the mutants and were associated with slower rates of CaM-dependent ferric heme reduction. However, a D1393V mutant whose flavins had been prereduced with NADPH had a normal rate of heme reduction. This indicated that the kinetic defect was restricted to flavin reduction step(s) in the mutants and suggested that this limited their catalytic activities. Together, our results show the following. 1) The presence and positioning of the Asp-1393 carboxylate side chain are critical to enable NADPH-dependent reduction of the nNOS flavoprotein. 2) Control of flavin reduction is important because it ensures that the rate of heme reduction is sufficiently fast to enable NO synthesis by nNOS.

Nitric oxide (NO)[1] is a widespread signal and effector molecule in biology (1–3). Animals generate NO by virtue of the nitric-oxide synthases (NOSs), which catalyze a stepwise, NADPH-dependent oxidation of L-Arg to NO and L-citrulline, with N^{ω}-hydroxy-L-arginine (NOHA) being formed as an intermediate. Each NOS is composed of an N-terminal oxygenase domain that binds iron protoporphyrin IX (heme), (6*R*)-tetrahydrobiopterin (H_4B), and substrate, L-Arg, and a C-terminal flavoprotein domain that binds FAD, FMN, and NADPH. A calmodulin (CaM)-binding sequence connects the oxygenase and flavoprotein domains. During catalysis, electrons from NADPH transfer into the FAD and FMN groups of the NOS flavoprotein domain, and then transfer one at a time from the FMN hydroquinone ($FMNH_2$) to the ferric heme (4–8) (Scheme 1).

Heme reduction enables the enzyme to bind O_2 and initiate an H_4B-dependent oxygen activation that is required for catalysis (9, 10). In all NOSs studied so far, the rates of NADPH-dependent flavin reduction are fast relative to the rates of electron transfer from $FMNH_2$ to the ferric heme in the CaM-bound enzymes (11–14). This makes heme reduction rate-limiting for NO synthesis and implies that the NOS flavins predominantly exist in their reduced forms during steady-state NO synthesis.

NOSs are part of a small enzyme family whose members have covalently linked flavoprotein and heme domains. The attached heme domain makes NOSs particularly useful for studying how electron transfer is regulated both into and out of the flavoprotein domain. NOS electron transfer reactions appear to be regulated at multiple levels by CaM. For example, CaM has been reported to increase the rates of NADPH-dependent flavin reduction and inter-flavin electron transfer, to increase the rate of electron transfer from the NOS flavoprotein to external acceptors like ferricyanide or cytochrome *c*, and to trigger NOS ferric heme reduction (14–18). These features are an important part of the unique regulation in NOS enzymes (19, 20).

The NOS flavoprotein domain is structurally and catalytically similar to other dual-flavin oxidoreductases like cytochrome P450 reductases, methionine synthase reductase, novel reductase-1 (NR-1), the flavoprotein subunit of sulfite reductase, and the flavoprotein domain of cytochrome P450BM3 (21–25). In these enzymes, the NADPH and FAD binding regions actually represent a ferredoxin NADP$^+$ reductase-like module (FNR) that is also found in transhydrogenase enzymes including ferredoxin-NADP$^+$ reductase, NADH-nitrite reductase, and NADH-cytochrome b_5 reductase (21–32). Sequence comparisons and crystallographic studies have identified some common structural motifs that participate in dinucleotide cofactor binding or impact electron transfer in the FNR-like enzymes. For example, there typically are three conserved residues positioned near the NAD(P)H-FAD interface in these enzymes. These residues are represented in rat nNOS by Asp-

* This work was supported by National Institutes of Health Grant GM51491 (to D. J. S.) and a grant from The American Heart Association (to S. A.). The costs of publication of this article were defrayed in part by the payment of page charges. This article must therefore be hereby marked "*advertisement*" in accordance with 18 U.S.C. Section 1734 solely to indicate this fact.

‡ Both authors contributed equally to this work.

§ Present address: Dept. of Infectious Disease, Indian Institute of Chemical Biology, 4, Raja S.C. Mullick Rd., Calcutta-700032, India.

¶ To whom correspondence should be addressed: Immunology NB-30, Lerner Research Institute, Cleveland Clinic, 9500 Euclid Ave., Cleveland, OH 44195. Tel.: 216-445-6950; Fax: 216-444-9329; E-mail: stuehrd@ccf.org.

[1] The abbreviations used are: NO, nitric oxide; NOS, nitric-oxide synthase; nNOS, neuronal NOS; NOHA, N^{ω}-hydroxy-L-arginine; CaM, calmodulin; H_4B, (6*R*)-tetrahydrobiopterin; CYPR, NADPH-cytochrome P450 reductase; FNR, ferredoxin NADP$^+$ reductase; EPPS, 4-(2-hydroxyethyl)-1-piperazinepropanesulfonic acid; $FMNH_2$, FMN hydroquinone.

SCHEME 1. **Path of electron transfer in nNOS.**

1393, Ser-1176, and Cys-1349 (27). Mutagenic substitution studies on the analogously positioned residues in FNR enzymes, cytochrome P450 reductase, and other related enzymes have established that each of the three residues helps to enhance the rate of hydride transfer between NAD(P)H and FAD (32–40). Given the structural and regulatory properties of the NOSs, we sought to examine how one of these conserved residues (Asp-1393, Fig. 1) functions in rat nNOS regarding NADPH reduction of the flavoprotein domain and its export of electrons. Crystal structures of some related flavoproteins have revealed that the carboxylate side chain of this conserved Asp makes hydrogen bonds with adjacent protein residues and with the nicotinamide moiety of NAD(P)H (20, 32, 40, 41). We therefore utilized site-directed mutagenesis to substitute Val, Asn, or Glu for Asp-1393 in nNOS. These either remove the side chain carboxylate, neutralize its charge, or alter its positioning, respectively. Characterization of these mutants reveals how Asp-1393 influences electron transfer into the nNOS flavoprotein domain, and how this in turn impacts electron transfer to the nNOS heme as well as the various catalytic activities.

EXPERIMENTAL PROCEDURES

Materials—All reagents and materials were obtained from Sigma or sources previously reported (16, 42, 43).

Molecular Biology—Restriction digestions, cloning, bacterial growth, and transformation and isolation of DNA fragments were performed using standard procedures. Originally, rat nNOS DNA was inserted into the 5′ NdeI and 3′ XbaI site into the pCWori vector (16). The D1393V, D1393E, and D1393N mutation sites in the nNOS cDNA were constructed by subcloning a PCR-generated fragment from pCWori/nNOS using a 5′-oligonucleotide containing a newly engineered mutational site. The nNOS cDNA fragment coding from the KpnI unique restriction site at 4176 to the XbaI restriction site at 4441 was amplified using primers as follows: D1393V forward primer, AACGGTACCACGAG**GTC**ATCTTTGGAGTCACCCTCAGAA, and D1393V reverse primer, AAATCTAGAAGGACCAGGACACAGCAACAGGACAAG; D1393E forward primer, AACGGTACCACGAG**GAA**ATCTTTGGAGTCACCCTCAGAA, and D1393E reverse primer, AAATCTAGAAGGACCAGGACACAGCAACAGGACAAG; and D1393N forward primer, AACGGTACCACGAG**AAC**ATCTTTGGAGTCACCCTCAGAA, and D1393N reverse primer, AAATCTAGAAGGACCAGGACACAGCAACAGGACAAG. The silent restriction sites and mutation sites are denoted by underlines and boldface, respectively. The PCR product and wild-type pCWori vector containing nNOS DNA were digested by both KpnI/XbaI restriction enzymes. The double digested fragment of wild-type NOS pCWori plasmid was replaced by the double digested PCR fragment and transformed into JM109 cells to generate recombinant plasmid. Sequences of mutations were confirmed at the Cleveland Clinic DNA Sequencing Facility. Plasmids containing D1393V, D1393E, or D1393N mutant DNA were transformed into *Escherichia coli* strain BL21(DE3) for protein expression.

Expression and Purification of Wild-type and Mutant Proteins—Wild-type rat nNOS and all three mutant proteins had a His_6 tag attached to their N termini to aid purification. They were overexpressed in *E. coli* strain BL21(DE3) and purified by sequential chromatography on Ni^{2+}-nitrilotriacetic acid and 2′,5′-ADP-Sepharose resins in the absence of CaM as described earlier (16, 42).

Determination of Bound FAD and FMN—Bound FAD and FMN were released from nNOS or mutants by heat denaturation (95 °C for 5 min in the dark) and measured using a fluorometric high pressure liquid chromatography method as described previously (16).

NO Synthesis, NADPH Oxidation, Cytochrome c Reduction, and Ferricyanide Reduction—Steady-state activities of wild-type and mutant proteins were determined separately at 25 °C using spectrophotometric assays that were described previously in detail (16, 42, 43).

Measurement of Apparent K_m for NADPH—Apparent K_m and V_{max} values were determined by double-reciprocal analysis of the NADPH-dependent cytochrome *c* reductase activity *versus* initial NADPH concentration with reactions run in the presence or absence of Ca^{2+}/CaM.

Steady-state NADPH Oxidation—Wild-type and mutant nNOS enzymes were diluted to 4 μM in a cuvette that contained buffer, H_4B, Ca^{2+}, CaM, and other additives as used for the NO synthesis assay (42), except that here oxyhemoglobin, L-Arg, and NADPH were omitted. A spectrum was collected, and NADPH solution was then added to give 100 μM, and a second spectrum was collected during NADPH consumption.

Flavin and Heme Reduction Kinetics—Kinetics of flavin and heme reduction were analyzed at 10 °C as described previously (16, 42, 43) using a stopped-flow apparatus (with a dead time of 1.5 ms) from Hi-Tech Ltd. (models SF-61 and 51-MX) connected to diode array or single wavelength detectors and equipped for anaerobic work. Flavin reduction kinetics was determined from the absorbance change at 485 nm and in some cases at 600 nm. In the case of D1393V nNOS, the enzyme preparation to be used in flavin reduction experiments was first treated with $FeCN_6$ followed by size exclusion chromatography to oxidize the air-stable FMN semiquinone that is normally present in the enzyme after purification. The NOS heme reduction inhibitor *N*-nitro-L-arginine (44) was also added in order to prevent concurrent electron transfer from $FMNH_2$ to the ferric heme during measures of flavin reduction kinetics. In cases where the rate of heme reduction was to be determined, we omitted *N*-nitro-L-arginine. Heme reduction was monitored by formation of the ferrous-CO complex and the kinetics determined by fitting traces of absorbance change *versus* time at 444 nm. Unless stated otherwise, reactions were initiated by rapid mixing an anaerobic CO-saturated solution containing 100 μM NADPH with an anaerobic CO-saturated solution containing wild-type or mutant nNOS (2 μM), 40 mM EPPS buffer, pH 7.6, 10 μM H_4B, 0.3 mM dithiothreitol, 1 mM L-Arg, 4 μM CaM, and 1 mM Ca^{2+}. In one case, the heme reduction kinetics in D1393V nNOS was studied differently. The enzyme was preincubated at room temperature with excess NADPH in an anaerobic cuvette and in the absence of CaM and added Ca^{2+}, in order to prereduce the flavoprotein domain. NADPH reduction of enzyme flavins was confirmed by monitoring the loss of absorbance between 380 and 500 nm *versus* time of preincubation, and took about 1 h. The prereduced enzyme was then transferred into the stopped-flow device and mixed under anaerobic conditions with a CO-saturated solution containing 1 mM Ca^{2+} and 4 μM CaM to trigger heme reduction. In all stopped-flow studies, the signal-to-noise ratios were improved by averaging 7–10 individual mixing experiments. The time course of absorbance change was fit to single or multiple exponential equations using a nonlinear least squares method provided by the instrument manufacturer.

Fluorescence Spectroscopy—Flavin fluorescence measurements were done using a Hitachi model F-2000 spectrofluorometer as described previously (42, 45). A 1-ml quartz cuvette with a path length of 1 cm was used for the experiments. The nNOS proteins were diluted to 2 μM in 40 mM EPPS, pH 7.6, containing 0.6 mM EDTA, 1 mM DDT, and 3 μM CaM. Proteins were irradiated with 460 nm light using an in-line 8% filter, and the emission at 530 nm was monitored *versus* time before and after consecutive addition of 1 mM Ca^{2+} and 3 mM EDTA.

RESULTS

Spectral and Physical Properties—The Asp-1393 mutant nNOS proteins expressed well in *E. coli* and displayed normal spectral properties in their purified forms. For example, the mutants exhibited a Soret peak at 393 nm and visible peaks at 460 and 485 nm in the presence of 1 mM L-Arg and 10 μM H4B (data not shown). Dithionite reduction of each mutant in the presence of L-Arg, H_4B, and CO produced the expected 444 nm absorbance peak for the six coordinate ferrous-CO complex in all cases (data not shown). Flavin analysis showed that the mutants contained normal quantities of FAD and FMN (~1 each per nNOS heme) (data not shown). Their ability to bind and elute from the 2′,5′-ADP resin during purification showed that they still could reversibly bind NADPH. These properties indicate that substitution of Asp-1393 by Val, Glu, or Asn did not grossly alter the physical properties of nNOS.

Steady-state Catalytic Activities—Tables I and II list values for four steady-state catalytic activities of the wild-type and mutant nNOS enzymes that were measured at 23 (room temperature) and 10 °C. The D1393V mutant had markedly lower ferricyanide and cytochrome *c* reductase activities compared with wild type in either the CaM-bound or CaM-free state. CaM binding only marginally increased the cytochrome *c* or ferricyanide reductase activities of D1393V nNOS. In contrast, the

E.coli SIR-FP	^{593} RYQR**D**VY
C.elegans MSR	^{675} QYIE**D**VWG
Spinach FNR	^{363} QWNV**E**VY
NR1(Human)	^{590} RFQT**E**TWA
P450BM3	^{1041}RYAK**D**VWAG
Rat CYPR	^{671} RYSL**D**VWS
Mouse iNOS	^{1116}RYHE**D**IFGAVFSYGAKKGSALEEPKATRL
Rat nNOS	^{1389}RYHE**D**IFGVTLATYEVTNRLRSESIAFIEESKKDADEVFSS
Bovine eNOS	^{1155}RYHE**D**IFGLTLRTQEVTSRIRTQSFSLQERHLRGAVPWAFDPPGPDTPGP

FIG. 1. **C-terminal protein sequence alignment for NOS enzymes and some related flavoproteins.** Residues that align with Asp-1393 are in *boldface. eNOS*, endothelial NOS; *iNOS*, inducible NOS.

TABLE I

Steady-state catalytic activities of wild-type and mutant nNOS

Reactions were run at room temperature. The NO synthesis rate was measured using L-Arg as substrate. Values are the means ± S.D. for three determinations and are representative of data obtained with two preparations of each enzyme. ND, non-detectable.

nNos enzyme	Ferricyanide reduction		Cytochrome *c* reduction		NO synthesis		NADPH oxidation	
	+CaM	−Cam	+CaM	−CaM	+CaM	−CaM	+CaM	−CaM
	min^{-1}		*min*$^{-1}$		*min*$^{-1}$		*min*$^{-1}$	
Wild type[a]	5182 ± 300	955 ± 32	5742 ± 116	462 ± 11	65 ± 1	ND	128 ± 4	5.6 ± 1
D1393E	1600 ± 104	500 ± 23	1082 ± 51	104 ± 5	21 ± 1	ND	54 ± 2	2.4 ± 0.1
D1393N	1701 ± 47	673 ± 16	1193 ± 28	127 ± 1	28 ± 2	ND	68 ± 3	2.8 ± 0.03
D1393V	12 ± 1	11 ± 1	10 ± 1	10 ± 1	ND	ND	0.5 ± 0.1	1 ± 0.1

[a] Data from Ref. 65.

TABLE II

Steady-state catalytic activities of wild-type and mutant nNOS at 10 °C

NO synthesis rate was measured using L-Arg as substrate. Values are the means ± S.D. for three determinations and are representative of data obtained with two preparations of each enzyme. ND, non-detectable.

nNos enzyme	Ferricyanide reduction		Cytochrome *c* reduction		NO synthesis		NADPH oxidation	
	+CaM	−Cam	+CaM	−CaM	+CaM	−CaM	+CaM	−CaM
	min^{-1}		*min*$^{-1}$		*min*$^{-1}$		*min*$^{-1}$	
Wild type	1767 ± 115	311 ± 23	1077 ± 83	85 ± 7	17.8 ± 1.6	ND	32 ± 1	1.8 ± 0.2
D1393E	432 ± 26	141 ± 11	207 ± 11	19 ± 1	6.1 ± 0.4	ND	15 ± 1	0.6 ± 0.03
D1393N	446 ± 31	156 ± 12	219 ± 5	20 ± 1	8.5 ± 0.6	ND	18 ± 1	0.7 ± 0.03
D1393V	3.9 ± 0.1	3.6 ± 0.2	2.0 ± 0.2	2.0 ± 0.1	ND	ND	ND	ND

D1393E and D1393N mutants had basal ferricyanide and cytochrome *c* reductase activities that ranged from one-fourth to one-half of the wild-type enzyme reductase activities. CaM increased the reductase activities of the D1393E and D1393N mutants in a manner similar to wild type, although the absolute values achieved for the mutants remained lower and ranged from one-fourth to one-third those of wild-type nNOS plus CaM.

CaM was obligatory for NO synthesis by D1393E and D1393N nNOS, and their activities were about one-third that of wild type at room temperature (Table I). In contrast, D1393V nNOS had no detectable NO synthesis when L-Arg was the substrate, but did show a low, detectable activity (1.3 ± 0.4 NO per min at room temperature) when the reaction intermediate NOHA was used as substrate in place of L-Arg. Rates of NADPH oxidation were also measured during the NO synthesis assays or in the absence of CaM (Tables I and II). For the D1393E and D1393N mutants, the NADPH oxidation rates were proportionally lower than that of wild-type nNOS. Thus, NADPH oxidation in these mutants remained relatively well coupled to their NO synthesis. Rates of NADPH oxidation for D1393V nNOS were much lower than those of wild-type nNOS, consistent with its poor NO synthesis. Together, the results indicate that the carboxyl side chain of Asp-1393 has a crucial role in the catalysis of these four steady-state activities in the presence or absence of CaM.

Apparent K_m for NADPH and Enzyme CaM Response—The apparent K_m values for NADPH in the nNOS mutant proteins did not differ significantly from wild type (Table III). Apparent K_m values were increased 1.5–2-fold by CaM binding, consistent with a previous report (46). These data suggest that the Asp-1393 mutations did not significantly alter NADPH binding interaction with nNOS.

CaM binding to nNOS increases its flavin fluorescence in a partially reversible manner (42, 44). As shown in Fig. 2, CaM binding to either the D1393V or D1393E mutants caused fluorescence increases that were similar to those observed with wild-type nNOS. These results suggest that CaM binds to the Asp-1393 mutants and induces normal protein conformational changes within the flavoprotein domain.

Kinetics of Flavin and Ferric Heme Reduction—To determine how the Asp-1393 mutations impact electron transfer in nNOS, we compared rates of NADPH-dependent flavin and ferric heme reduction in the enzymes. The reactions were initiated in a stopped-flow spectrophotometer at 10 °C by rapid-mixing enzymes with excess NADPH under anaerobic conditions, and the absorbance change was followed using either a diode array or single wavelength detector. Rates of flavin reduction were determined by monitoring the absorbance decrease at 485 nm, whereas rates of heme reduction were determined from the absorbance increase at 444 nm, which monitors formation of a ferrous heme-CO complex (42, 43). Rates derived from these experiments are listed in Table IV.

Averaged absorbance traces representing flavin and heme

TABLE III
Apparent K_m value of NADPH for wild type and mutant nNOS enzymes

Values were determined using the cytochrome *c* reductase assay at room temperature and are the means ± S.D. of three measurements each.

nNOS enzyme	K_m of NADPH	
	−CaM	+CaM
	μM	
Wild type	2.5 ± 0.5	4.8 ± 0.2
D1393E	1.0 ± 0.2	2.4 ± 0.4
D1393N	1.3 ± 0.1	2.6 ± 0.3
D1393V	2.9 ± 0.4	4.5 ± 0.7

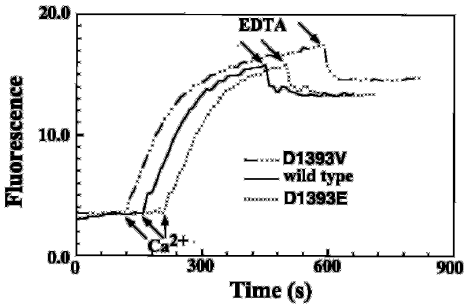

FIG. 2. **Flavin fluorescence change induced by CaM binding.** Ca^{2+} was added at the indicated time to induce CaM binding to each nNOS enzyme. Excess EDTA (3 mM) was then added to induce dissociation of CaM.

reduction in D1393E and D1393N nNOS are shown in Fig. 3, *A–C* and *D–F*, respectively. Like wild-type nNOS (15, 42), the absorbance change at 485 nm indicating flavin reduction was sufficiently described as biphasic for either mutant (Table IV), although less of their total absorbance change could be attributed to the fast phase as compared with wild-type enzyme. CaM increased the fast phase rates of flavin reduction for either mutant in a manner similar to wild-type enzyme.

The averaged kinetic traces obtained at 444 nm for the D1393E and D1393N mutants are displayed in Fig. 3, *C* and *F*. The initial decrease in absorbance that appears in both traces was due to the initial NADPH-dependent flavin reduction step that must take place prior to electron transfer to the ferric heme. The subsequent absorbance gain at 444 nm represents ferric heme reduction, and this phase was sufficiently described as a monophasic transition for both mutants. The data indicate that the rates of ferric heme reduction are similar for the D1393E and D1393N nNOS mutants and are about four times slower than in wild-type nNOS (Table IV).

In Fig. 4, *traces A* and *C* are the averaged absorbance traces recorded at 485 nm to follow flavin reduction in fully oxidized[2] D1393V nNOS in the presence or absence of CaM. The absorbance decrease at 485 nm was satisfactorily described as biphasic in both circumstances. Remarkably, flavin reduction in D1393V nNOS was about 1000 times slower than in wild-type enzyme (Table IV). The ability of CaM to increase the flavin reduction rate was also blunted in this mutant. However, CaM did cause a greater proportion of the total absorbance change at 485 nm to shift to the fast phase (Table IV), and also doubled the extent of flavin reduction that was achieved during the observation period, as judged by comparing the magnitude of absorbance decrease that was attained at 485 nm in the presence and absence of CaM (Fig. 4). Together, these results demonstrate that Asp-1393 exerts a powerful influence on the kinetics of NADPH-dependent flavin reduction and is also needed to obtain the full rate increase that is typically observed when CaM binds to nNOS.

We also followed the coincident absorbance change at 600 nm during NADPH-dependent flavin reduction of fully oxidized D1393V nNOS. Absorbance change at this wavelength can indicate the buildup and subsequent reduction of a flavin disemiquinone species that forms subsequently to hydride transfer from NADPH via a 1-electron transfer between FAD hydroquinone and FMN (Scheme 2) (15, 46). The averaged absorbance traces at 600 nm that were collected for the CaM-free and CaM-bound D1393V nNOS are shown in *traces B* and *D* of Fig. 4. After an ~5–10 s lag we observed an absorbance gain at 600 nm in both cases. This indicates that an inter-flavin electron transfer step occurred subsequent to hydride transfer from NADPH and led to the buildup of detectable amounts of a flavin di-semiquinone species in both the CaM-free and CaM-bound mutant enzyme, as also occurs in fully oxidized wild-type nNOS during its reduction with excess NADPH (15, 46). The 600 nm absorbance then remained constant in CaM-free D1393V nNOS over the rest of the observation period, whereas the absorbance decayed in the CaM-bound mutant. This result, together with the concurrent absorbance data recorded at 485 nm, indicates that CaM promotes reduction of the flavin disemiquinone species by a second molecule of NADPH in D1393V nNOS. The observed absorbance increases and decreases at 600 nm each fit well to a single exponential function. This gave calculated rates for the absorbance increases of $0.013 \pm 0.001\ s^{-1}$ (−CaM) and $0.048 \pm 0.006\ s^{-1}$ (+CaM), and for the absorbance decrease of $-0.0033 \pm 0.0003\ s^{-1}$ (+CaM only).

We next investigated the kinetics and extent of ferric heme reduction in D1393V nNOS enzyme preparations that either did or did not contain a residual air-stable FMN semiquinone that is typically present in the enzyme after purification. Samples of CaM-bound enzyme in a CO-saturated buffer were rapidly mixed with NADPH at 10 °C under anaerobic conditions in the stopped-flow instrument, and spectra were collected *versus* time as described earlier. The data from reaction of an enzyme preparation that contained residual FMN semiquinone is shown in Fig. 5, *A* and *B*. A significant degree of ferric heme reduction took place during the reaction period, as judged by the loss of ferric heme absorbance at 400 nm and coincident buildup of the heme ferrous-CO complex at 444 nm (Fig. 5*A*). In contrast, very little (about 5%) heme reduction took place over the same period in a control enzyme reaction that did not contain CaM (data not shown). This indicated that the heme reduction we observed in Fig. 5*A* represented CaM-dependent electron transfer between flavin and heme centers within D1393V nNOS, rather than an electron transfer through disproportionation of enzyme molecules in solution. Fig. 5*B* and *inset* depict the kinetics of heme reduction after mixing a CaM-bound D1393V nNOS with excess NADPH. Heme reduction was delayed for about 15 s and was then biphasic, such that there was a 40-fold difference between the fast and slow rates of absorbance increase at 444 nm (Table IV).[3] The proportion of absorbance gain attributed to the fast phase ranged from 70 to 25% among three D1393V nNOS preparations (data not shown). Remarkably, the fast phase of heme reduction in

[2] Fully oxidized D1393V nNOS refers to an enzyme preparation that had been treated with $FeCN_6$ followed by size exclusion chromatography to oxidize the air-stable FMN semiquinone that is normally present in the enzyme after purification. The NOS heme reduction inhibitor *N*-nitro-L-arginine (44) was also present during measurement of NADPH-dependent flavin reduction kinetics in this mutant. See "Experimental Procedures" for details.

[3] The rate of heme reduction was corrected to take into account a coincident loss of absorbance at 444 nm that takes place due to the slow flavin reduction in D1393V nNOS.

TABLE IV
Observed rates of flavin and heme reduction in wild-type and mutant nNOS

Measurements were made under anaerobic conditions at 10 °C as described under "Experimental Procedures." The values are the means ± S.D. of 7–10 individual reactions and are representative of experiments done with two enzyme preparations each. Values in parentheses are the percentage of absorbance change attributed to each phase.

Step	nNOS protein			
	Wild type	D1393E	D1393N	D1393V
			s^{-1}	
Flavin reduction −CaM				
k_1	6.2 ± 0.7 (60%)	2.5 ± 0.8 (48%)	3.8 ± 0.1 (43%)	0.028 ± 0.001 (37%)
k_2	0.71 ± 0.07 (40%)	0.39 ± 0.09 (52%)	0.33 ± 0.04 (57%)	0.0016 ± 0.0003 (63%)
Flavin reduction + CaM				
k_1	48 ± 1.8[a]	11 ± 3.1 (51%)	12 ± 1.2 (53%)	0.045 ± 0.002 (66%)
k_2	4.2 ± 0.3[a]	4.0 ± 1.0 (49%)	2.4 ± 0.8 (47%)	0.0064 ± 0.0006 (34%)
Heme reduction + CaM				
k_1	4.6 ± 0.2[a]	1.1 ± 0.06 (100%)	1.3 ± 0.08 (100%)	0.033 ± 0.003 (70%)
k_2				0.0008 ± 0.0004 (30%)

[a] Data taken from Ref. 65.

D1393V nNOS was still 200 times slower than the heme reduction rate in wild-type nNOS (Table IV).

To examine whether the residual flavin semiquinone that was present in the D1393V nNOS preparation was linked to the biphasic heme reduction, we measured the kinetics of heme reduction in a CaM-bound D1393V nNOS preparation whose residual FMN semiquinone had been oxidized by $FeCN_6$ treatment prior to its reaction with NADPH in the stopped-flow spectrophotometer. Fig. 5*C* contains the averaged absorbance trace recorded at 444 nm during NADPH reduction of the preoxidized enzyme. After an initial delay, we observed a small absorbance gain whose rate matched the fast phase of heme reduction (data not shown) and thus may be attributed to the presence of a residual enzyme population that still contained a flavin semiquinone. There then was a further time delay before the bulk of heme reduction was initiated. This was essentially monophasic and proceeded at a rate of 0.0014 ± 0.0001 s^{-1}, which is similar to the slow phase rate of heme reduction that we obtained for the enzyme preparation used in Fig. 5*B*. Together, the results indicate that D1393V nNOS exhibits a shorter lag period and fast phase of heme reduction when it contains an air-stable flavin semiquinone, and exhibits a longer lag period and slow phase of heme reduction when it is fully oxidized.

We next wished to view the redox states of the flavins and heme during steady-state NADPH oxidation by the CaM-bound, H_4B-saturated enzymes in the absence of L-Arg.[4] Under this circumstance, electron transfer occurs from NADPH to FAD to FMN to heme to O_2. In addition, both O_2 binding and decay of the resulting heme ferrous-dioxy species are rapid in air-saturated buffer relative to the rate of heme reduction (47). These conditions enabled us to judge buildup of reduced flavins or heme during steady-state NADPH oxidation by simply comparing the spectra recorded before and during the reaction. Fig. 6 contains spectra recorded for each of the four H_4B-replete, CaM-bound proteins in both their resting ferric state and during steady-state NADPH oxidation in air-saturated buffer at room temperature. Spectra of wild-type nNOS indicate that its flavins exist in an almost completely reduced state during NADPH oxidation, along with a minor amount of reduced heme, the latter as judged by the partial decrease in ferric absorbance at 650 nm. This result matches what was reported previously for wild-type nNOS (48). The spectra of the D1393E and D1393N mutants indicate that their flavins exist only in a partly reduced state during NADPH oxidation (44 and 46% reduced relative to wild-type nNOS, respectively), as judged by comparing their absorbance decreases at 485 nm with wild type. There was no detectable buildup of ferrous heme in these enzymes. Finally, the spectra of D1393V nNOS show that its flavins are predominantly in the fully oxidized state during steady-state NADPH oxidation. These results indicate that different steps in the electron transfer cascade are rate-limiting among the enzymes.

We next examined if the Asp-1393 mutations impact electron transfer from $FMNH_2$ to the ferric heme. We measured the rate of ferric heme reduction in a D1393V nNOS sample whose flavoprotein had been prereduced with NADPH. We preincubated the CaM-free mutant with excess NADPH under anaerobic conditions for ~1 h until maximal flavin reduction was achieved. The degree of flavin reduction obtained is indicated by the initial and final spectra that we recorded during the enzyme incubation with NADPH (Fig. 7, *inset*). We then mixed the prereduced enzyme with an anaerobic, CO-saturated buffer containing Ca^{2+} and CaM in the stopped-flow instrument, and we collected spectra to observe heme reduction as indicated by CO binding. In such an experiment, a rapid binding of CaM occurs upon mixing and triggers ferric heme reduction (17, 43). Fig. 7, *main panel*, contains the averaged kinetic trace collected at 444 nm during the reaction. There was a very rapid absorbance increase during the first 20 ms. The rate of this transition suggests that it represents CO binding to an enzyme fraction that had become reduced to ferrous during the incubation with NADPH.[5] On the basis of the absorbance increase during this initial phase, we estimate that this reaction involved 30–40% of the total enzyme that was present in the sample. The next portion of the 444 nm trace was a monophasic absorbance increase that indicated ferric heme reduction as triggered by CaM binding. The calculated rate of this phase was 4.9 ± 0.3 s^{-1}, which is essentially equivalent to the rate of ferric heme reduction that we measured in wild-type nNOS (Table IV). These results indicate that the flavoprotein domain of D1393V nNOS functions normally in catalyzing electron transfer between $FMNH_2$ and the ferric heme.

DISCUSSION

Our results confirm that Asp-1393 enables flavin reduction by NADPH and reveal how this effect impacts downstream electron transfer events and catalytic activities of nNOS. The site-directed substitutions at Asp-1393 appeared to be well tolerated by nNOS because the mutants had normal flavin content, NADPH interaction, and flavin fluorescent response

[4] L-Arg is omitted to prevent NO generation during catalysis, because otherwise the NO will quickly bind to the enzyme and cause prominent buildup of heme-NO species (48) that confound the spectral analysis.

[5] The heme reduction occurred in CaM-free nNOS due to a slow electron transfer between enzyme molecules in solution.

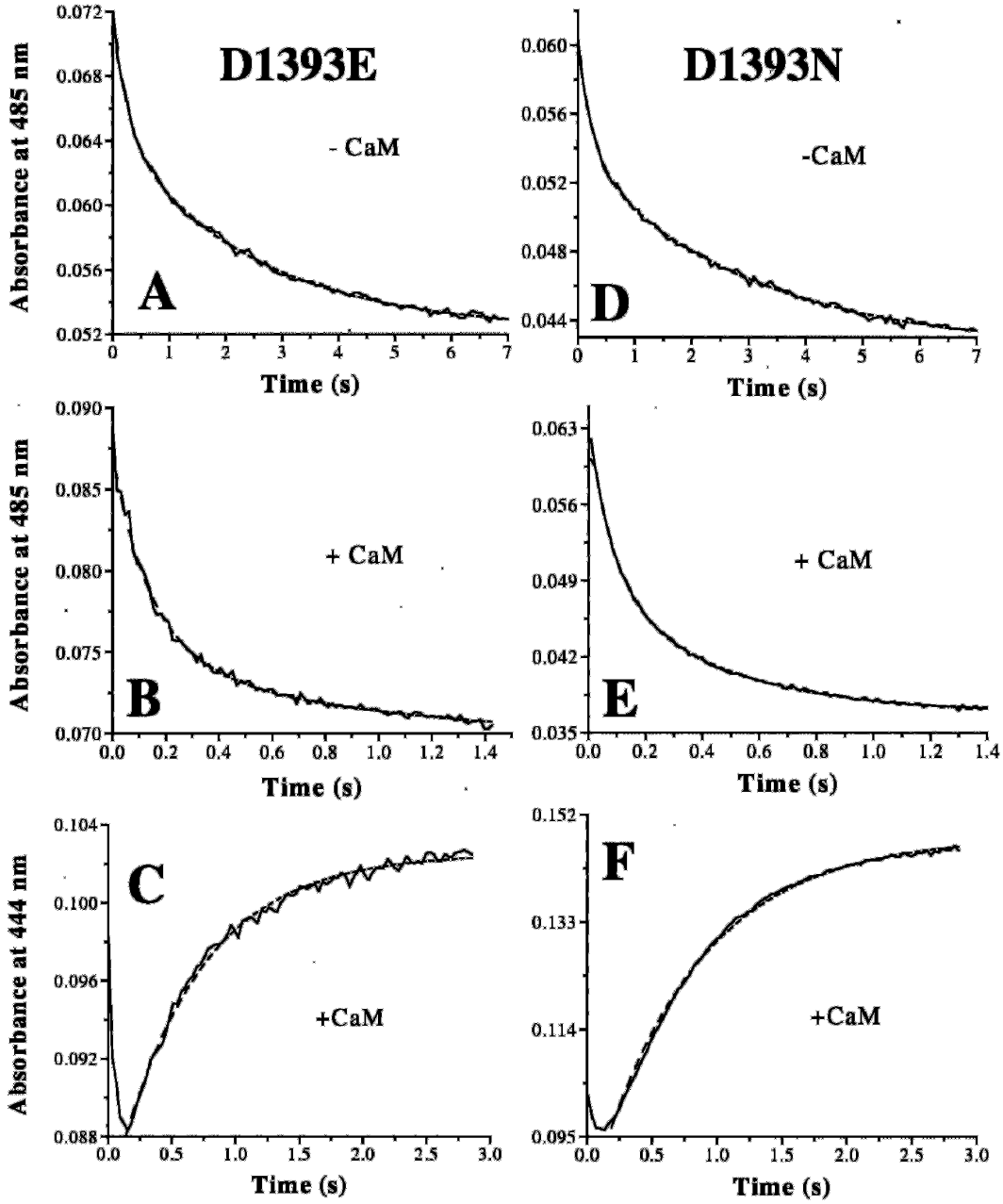

FIG. 3. **Kinetics of flavin and heme reduction in D1393E and D1393N nNOS at 10 °C.** D1393E (*A–C*) and D1393N (*D–F*) were rapidly mixed with excess NADPH under anaerobic conditions in a stopped-flow spectrophotometer to initiate the reaction. *A* and *D* and *B* and *E* depict the time-dependent absorbance loss at 485 nm associated with flavin reduction in the CaM-free or CaM-bound enzymes, respectively. *C* and *F* show the time-dependent increase in absorbance at 444 nm that is associated with heme reduction as determined by CO binding to the CaM-bound enzymes. Each panel contains a solid averaged absorbance trace and a *dashed calculated line* of best fit.

upon CaM binding. This is consistent with CYPR and FNR enzymes tolerating similar mutations made at the homologous residue (35, 37). The specific nature of the Asp-1393 mutations allowed us to examine how they impact flavin reduction and catalytic events such as cytochrome *c* reduction, nNOS heme reduction, and NO synthesis.

Flavin Reduction—Steps involved in flavin reduction by excess NADPH have been described for CYPR and related enzymes (18, 35, 46, 49, 50). After NADPH binds it quickly forms a charge transfer complex with FAD and then engages in a relatively rapid hydride transfer to FAD. Subsequent steps include inter-flavin electron transfer, release of $NADP^+$, binding of a second NADPH molecule, and further electron transfer into and among the flavins. A biphasic absorbance loss at 485 nm has been reported previously to describe NADPH-dependent flavin reduction in wild-type nNOS (11, 16, 43) and in CYPR (35, 50). In general, the first phase is thought to correspond to hydride transfer to FAD and rapid inter-flavin electron transfer, whereas the second phase has been proposed to correspond to further reduction of the flavins by a second molecule of NADPH and to potentially be rate-limited by $NADP^+$ release and/or some conformational change (18). However, another group has suggested that the slower phase could also represent inter-flavin electron transfer from FAD to FMN (15, 46).

Each of our Asp-1393 mutants exhibited biphasic absorbance loss at 485 nm when reacted with excess NADPH, and CaM increased the rates in all cases. This indicates that the mutants

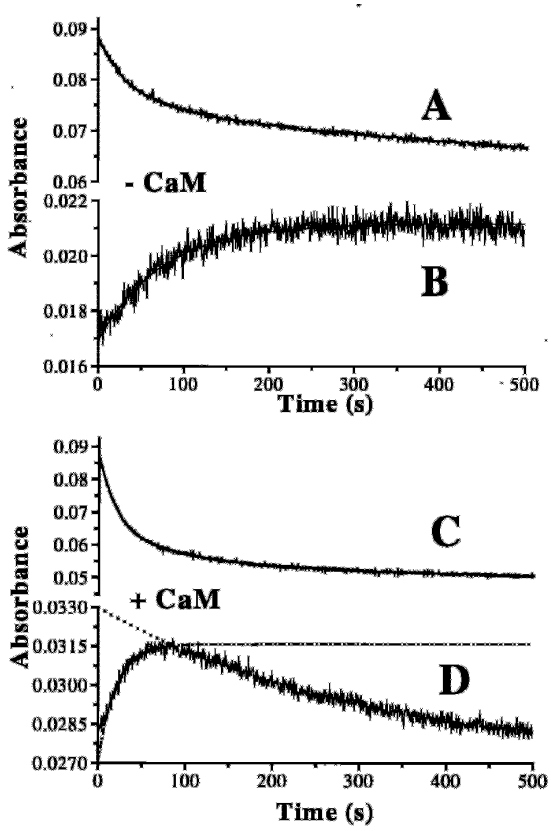

FIG. 4. **Kinetics of flavin reduction in D1393V nNOS at 10 °C.** Enzyme samples were rapidly mixed with excess NADPH under anaerobic conditions in a stopped-flow spectrophotometer to initiate the reaction. The figure contains averaged absorbance traces from 8 to 10 individual scans that indicate the time-dependent changes occurring at 485 and 600 nm for the CaM-free enzyme (*traces A* and *B*) and for the CaM-bound enzyme (*traces C* and *D*). *Solid* (*traces A–C*) or *dashed* (*trace D*) *calculated lines* of best fit are included.

SCHEME 2. **Distribution of NADPH-derived electrons in the nNOS flavoprotein domain.**

have a normal CaM response, at least regarding its ability to kinetically enhance the steps involved in NADPH-dependent flavin reduction.

The absorbance traces collected at 600 nm help to extend these results for D1393V nNOS. Within the first 5–10 s of NADPH reaction with the CaM-bound mutant, there was no significant absorbance gain at 600 nm despite some absorbance loss at 485 nm within the same period (about 25% of the total loss at 485 nm). This suggests that NADPH bound, and perhaps some hydride transfer occurred in the enzyme prior to the start of inter-flavin electron transfer. Next, during the 10–50-s reaction period the flavin reduction rate as judged by absorbance loss at 485 nm (k_1, fast phase) was approximately equivalent to the buildup rate of flavin semiquinone species as judged by the absorbance gain at 600 nm, indicating a period where hydride transfer to FAD occurred coincident with inter-flavin electron transfer. Finally, during the 50–500-s reaction period the rate of flavin reduction measured at 485 nm (the slow phase or k_2) became approximately equivalent to the decay rate of the flavin semiquinone species as judged at 600 nm, suggesting a period of further flavin reduction by a second molecule of NADPH. The ability of CaM to speed the processes that enable flavin reduction by a second molecule of NADPH was particularly apparent in D1393V nNOS, because only in its

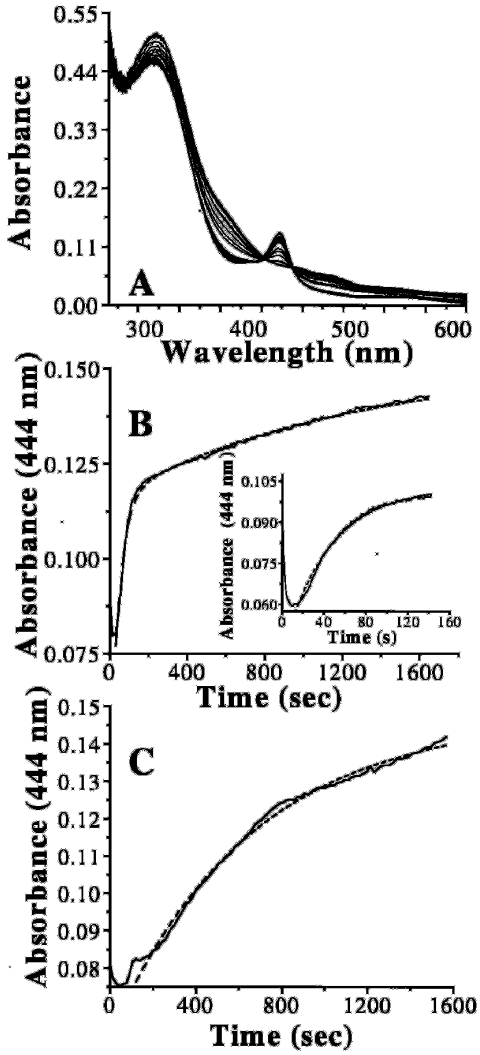

FIG. 5. **Kinetics of heme reduction in D1393V nNOS at 10 °C.** Heme reduction was monitored by measuring the formation of the enzyme ferrous-CO complex. *A* contains selected rapid-scanning spectra that were recorded within 24 min after mixing excess NADPH (100 μM) with 2 μM CaM-bound D1393V nNOS under anaerobic conditions in a stopped-flow spectrophotometer. *B* and *C* contain averaged absorbance traces at 444 nm (8–10 individual scans each) from experiments that used an enzyme preparation that contained residual flavin semiquinone (*B* and *inset*) or an enzyme preparation whose residual flavin semiquinone was oxidized by pretreatment with $FeCN_6$ (*C*). The *dashed lines* of best fit are included.

CaM-bound state did we observe coincident decay of the flavin semiquinone signal and further absorbance loss at 485 nm within the 500-s data collection period. This result suggests that CaM facilitates $NADP^+$ release from the enzyme, inter-flavin electron transfer, and/or hydride transfer from a second molecule of NADPH. In general, the kinetic effects that we observed for CaM in D1393V nNOS match what has been reported over much shorter time frames in experiments done with wild-type nNOS (15).

Our results imply that the inter-flavin electron transfer step is not rate-limiting for flavin reduction in D1393V nNOS. This derives from our observing nearly equivalent rates of flavin semiquinone buildup and flavin reduction in both the CaM-free and CaM-bound forms of this mutant. In addition, the spectrum recorded during NADPH oxidation by CaM-bound D1393V nNOS showed that very little reduced flavin species build up during the steady state. Thus, hydride transfer from NADPH to FAD appears to limit the rate of flavin reduction in this mutant.

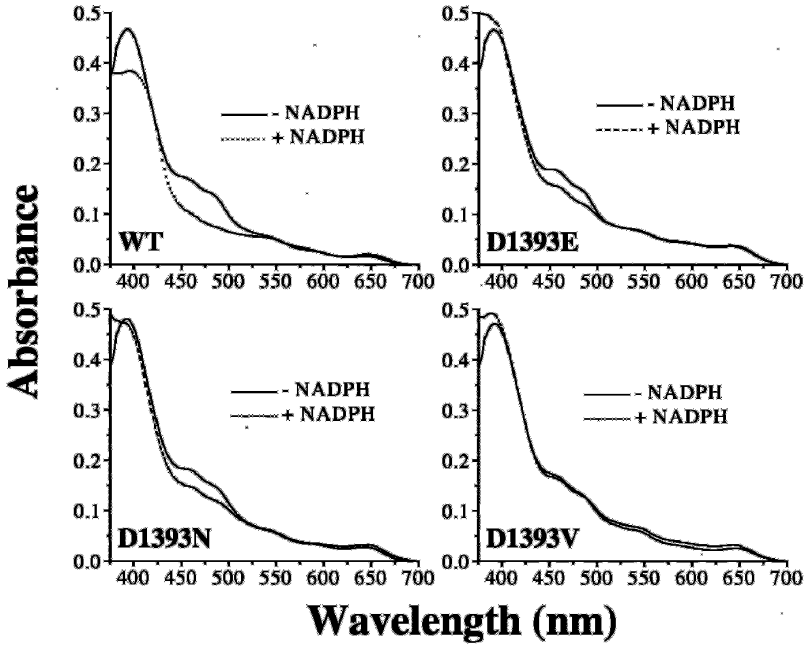

FIG. 6. **Redox states of enzyme flavin and heme centers during steady-state NADPH oxidation.** Wavelength scans of wild-type nNOS and each Asp-1393 mutant enzyme were recorded before (*solid line*) and after (*dashed line*) initiating the reaction with 100 μM NADPH at room temperature. Scans are representative of three independent experiments done under identical conditions.

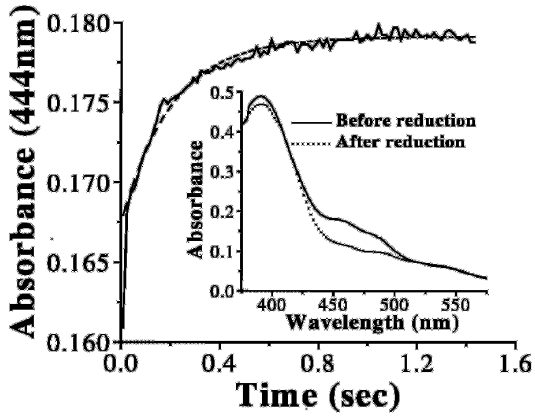

FIG. 7. **Kinetics of heme reduction at 10 °C for a D1393V nNOS that contains a prereduced flavoprotein domain.** A preparation of D1393V nNOS had been prereduced by incubation with excess NADPH (100 μM) prior to the stopped-flow experiment. The *inset* contains wavelength scans of the enzyme preparation before (*solid line*) and after (*dashed line*) preincubation with NADPH. The *main panel* contains an averaged absorbance trace (8 individual scans) for a reaction in which the NADPH preincubated enzyme was mixed in the stopped-flow instrument with a solution containing excess Ca^{2+} and CaM to trigger heme reduction. A *dashed line* of best fit is included.

Cytochrome c Reduction—It is useful to consider how the rates of flavin reduction in our Asp-1393 mutants and wild-type nNOS compare with their steady-state rates of electron transfer to cytochrome *c*. In CaM-bound D1393V nNOS, the initial rate of flavin reduction (k_1 at 485 nm) is approximately equivalent to the inter-flavin electron transfer rate (as judged by the rate of absorbance increase at 600 nm), which in turn is approximately equivalent to the rate of cytochrome *c* reduction (about 0.03 s^{-1} at 10 °C). However, this relationship between the fast phase of flavin reduction (k_1 at 485 nm) and rate of cytochrome *c* reduction does not hold for the wild-type nNOS or for the D1393E and D1393N mutants. In either their CaM-bound or CaM-free states, the k_1 values for flavin reduction are between 4 and 10 times faster than the rates of cytochrome *c* reduction at 10 °C. In fact, for the D1393E and D1393N mutants, the rates of cytochrome *c* reduction better match the slow phase of their flavin reduction (k_2 at 485 nm). As noted above, the value of k_2 likely relates to events that are subsequent to the initial hydride transfer step but are still critical for $FMNH_2$ formation during the steady state, including $NADP^+$ release, inter-flavin electron transfer, and further reduction by NADPH. To conclude, the analysis suggests that hydride transfer limits the rate of cytochrome *c* reduction by D1393V nNOS, whereas a subsequent step (or steps) involved in flavin reduction limits the rate of cytochrome *c* reduction by wild-type nNOS and by the D1393E and D1393N mutants.

Heme Reduction—In wild-type nNOS, flavin reduction is faster than ferric heme reduction and so heme reduction limits the rate of NO synthesis (11–14, 51). NOS heme reduction requires $FMNH_2$ formation because only this species can transfer an electron to the ferric heme in the CaM-bound enzyme (52, 53). Thus, by virtue of an attached heme domain, nNOS has a built-in indicator of FMN redox status that is absent in simpler flavoproteins like CYPR.

In D1393V nNOS we observed two rates of heme reduction, with the fast and slow phases being associated with enzyme subpopulations that as isolated either did or did not contain an electron in the flavoprotein domain, respectively. We also observed two different lag periods for heme reduction, with the shorter lag time being associated with the 1-electron-reduced enzyme subpopulation. These results can be understood by considering Fig. 8, which illustrates how NADPH-derived electrons may load into a fully oxidized *versus* 1-electron-reduced form of the nNOS flavoprotein. The midpoint reduction potentials of the nNOS flavins are known (53) and indicate that two NADPH binding and hydride transfer events are needed to generate significant amounts of $FMNH_2$ when starting with the fully oxidized flavoprotein. However, when starting with the 1-electron reduced form, a single hydride transfer from an NADPH is sufficient to generate significant amounts of $FMNH_2$. Thus, upon mixing a CaM-bound, fully oxidized D1393V nNOS with excess NADPH, there was about a 150-s lag period before initiating the slow phase of heme reduction. The long delay and slow rate of heme reduction under this circumstance (0.001 s^{-1}) match our estimates for the delay time and rate of flavin semiquinone reduction by a second molecule of NADPH as is required to generate significant amounts of $FMNH_2$ in the fully oxidized enzyme. Indeed, the data in Fig. 4 indicate that flavin semiquinone reduction by a second NADPH begins about 100 s after mixing and proceeds at

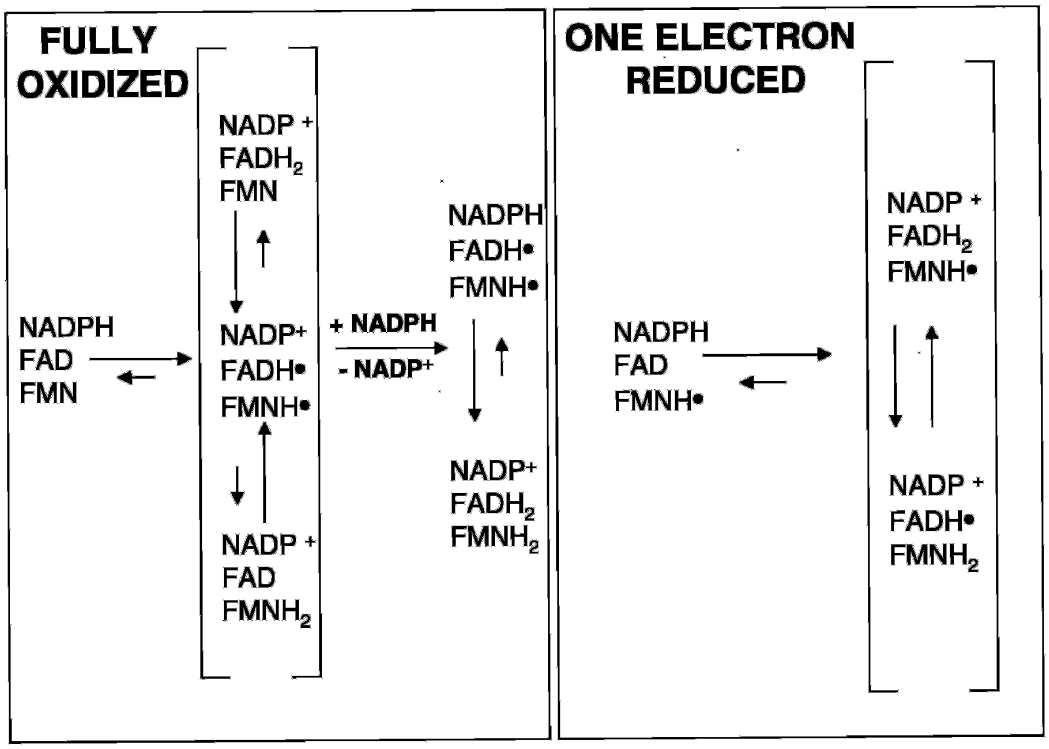

FIG. 8. **Possible electron distribution patterns during NADPH reduction of a fully oxidized (*left*) *versus* 1-electron-reduced (*right*) nNOS reductase domain.** Not all possible species are shown. Comparative *arrow lengths* indicate the direction of the thermodynamic equilibrium as based on the measured flavin midpoint potentials for nNOS (53).

a rate of about 0.003 s^{-1}. In contrast, for NADPH reduction of the 1-electron-reduced D1393V nNOS, there was a shorter lag time (about 20 s) and about a 10-fold faster rate of ferric heme reduction (0.03 s^{-1}). These timings correlate well with our estimated delay time and rate of hydride transfer between an initial molecule of NADPH and FAD (15-s delay, 0.045 s^{-1}). To conclude, the kinetic data for D1393V nNOS indicate that hydride transfer from NADPH limits the rate of all subsequent electron transfer steps in this mutant. It is likely that the different lag times and rates of heme reduction that we observed in the 0- and 1-electron-reduced forms of D1393V nNOS are due to the enzyme requiring two *versus* one molecule of NADPH, respectively, to achieve significant $FMNH_2$ formation. However, once $FMNH_2$ is formed in D1393V nNOS, it seems capable of reducing the ferric heme at a normal rate, as judged from our stopped-flow heme reduction experiment using an NADPH prereduced enzyme that contained $FMNH_2$.

A different situation exists in the D1393N and D1393E mutants. The spectra collected during their steady-state NADPH oxidation showed that their flavins are maintained in about a 50% reduced state along with an oxidized (ferric) heme. Given the linear path of electron transfer in nNOS (*i.e.* NADPH to FAD to FMN to heme), this result can only mean that the slow step in the electron transfer pathway is downstream from hydride transfer but before the electron transfer from $FMNH_2$ to heme. Indeed, in a case where electron transfer between $FMNH_2$ and ferric heme is rate-limiting (as occurs in wild-type nNOS), one observes near-complete flavin reduction during the steady state. Thus, we can conclude that hydride transfer between NADPH and FAD is not rate-limiting for heme reduction in D1393E and D1393N nNOS. This concept is also supported by their fast phase rates of flavin reduction (k_1 values at 485 nm) being at least 3-fold greater than their rates of cytochrome *c* reduction, which also depends on the rate of $FMNH_2$ formation.

Given the above, can we discern if the rate of $FMNH_2$ formation in D1393N and D1393E nNOS limits their rate of ferric heme reduction? This would be consistent with the mutants having longer lag times before initiating NADPH-dependent heme reduction in the stopped-flow experiments (they had lag times of about 160 ms compared with 30 ms for wild type). Three other types of data can address this question. On one hand, we have their estimated rates for steady-state cytochrome *c* reduction at 10 °C (3.4 and 3.6 s^{-1}). These are close to but still a bit faster than the observed rates of heme reduction at 10 °C for these mutants (1.1 and 1.3 s^{-1}). On the surface, this comparison suggests that other factors besides the rate of $FMNH_2$ formation may help to limit the rate of heme reduction. On the other hand, we have the steady-state spectral traces that indicate very little if any $FMNH_2$ builds up in these two mutants during their NADPH oxidation (if it did build up, we would have observed greater than 50% flavin reduction in the steady state). Moreover, once $FMNH_2$ is formed in D1393V nNOS, it supports a normal rate of electron transfer to the heme upon CaM binding, which implies that this specific electron transfer step is not affected by the Asp-1393 mutations. Thus we believe the balance of evidence is consistent with the rate of heme reduction in D1393N and D1393E nNOS being limited by the rate of $FMNH_2$ formation. The basis for this effect is under further investigation.

NO Synthesis—The lower NO synthesis activities of D1393E and D1393N nNOS are expected given their slower rates of heme reduction, as established previously with wild-type nNOS (16, 54). One may note that the percent decrease in NO synthesis activity of these mutants (about 35–45% slower than wild-type nNOS) is less than the percent decrease in their heme reduction rates (about 75% slower than wild type). This apparent discrepancy is due to the complex way that the rate of heme reduction affects the relative importance of two other enzyme kinetic parameters that together determine the rate of NO release by nNOS during steady-state catalysis (16, 19).

The D1393V mutant had no detectable NO synthesis from L-Arg but did catalyze a slow rate from NOHA. This arises

because when the substrate is L-Arg the NOS heme must catalyze two sequential and independent rounds of oxygen activation to generate NO. Specifically, the first round is needed to convert L-Arg to NOHA, whereas the second round is needed to convert NOHA to NO plus citrulline. Each round requires that $FMNH_2$ be formed to transfer one electron to the ferric heme. Apparently, the regeneration rate of $FMNH_2$ is so slow in D1393V nNOS that the bound NOHA intermediate dissociates from the enzyme before it can be further oxidized. This behavior is consistent with the estimated NOHA dissociation rate from NOS (estimated k_{off} is from 1 to 3 s^{-1}; see Refs. 55–57). On the other hand, when NOHA is the substrate, only one $FMNH_2$ needs to form and transfer an electron to the heme to initiate the single round of oxygen activation that is required to generate NO (47).

Possible Structural Basis for Asp-1393 Function—Asp-1393 is part of a triad of residues in nNOS (Ser-1176, Cys-1349, and Asp-1393) that is conserved throughout the FNR enzyme family and has been shown in some members to enable reduction of their bound flavin by NAD(P)H (33–38). A crystal structure of the FNR subdomain of nNOS showed that Asp-1393 and the two other residues of the triad are positioned as in related flavoproteins to facilitate hydride transfer to FAD (27). How the conserved Asp may function at a molecular level was revealed in crystal structures of CYPR and FNR that contain NADP(H) with its nicotinamide ring held in either a "productive" or "non-productive" conformation (21, 32, 40, 41). In the productive conformation the nicotinamide ring is held up against the isoalloxazine ring of FAD to enable hydride transfer between them, whereas in the non-productive conformation the nicotinamide ring is displaced away from the FAD ring. The two conformations reveal two separate roles for the conserved Asp. In the productive conformation its side chain carboxylate forms a hydrogen bond with the nicotinamide to help properly position it against the FAD isoalloxazine ring. In the non-productive conformation the Asp carboxylate makes hydrogen-bonding interactions with neighboring Ser and Cys residues that are thought to enable proton transfer from solvent to the N-5 atom of the reduced FAD. The Asp carboxylate is also held close enough to the FAD to possibly influence the flavin mid-point reduction potentials.

In general, the available biochemical and structural data suggest that Asp-1393 performs similar functions in nNOS. To give just one example, the slow flavin reduction rates that we observed for our D1393V and D1393N nNOS mutants match remarkably well to the kinetic profiles of the analogous CYPR Asp-675 mutants (35). Similar function may extend to the two other residues of the nNOS triad, as a preliminary report has shown that Ser-1176 is important for cytochrome *c* reduction and NO synthesis (58). Thus, the available data suggest potential mechanisms whereby eliminating the carboxylate side chain of Asp-1393 (D1393V nNOS), altering its location (D1393E nNOS), or neutralizing its charge (D1393N nNOS) could each negatively impact hydride transfer from NADPH to FAD and slow electron transfer in the nNOS flavoprotein.

Role in the Regulatory Mechanisms of nNOS—The influence of Asp-1393 appears to be primarily restricted to NADPH reduction of the nNOS flavoprotein. This is an important distinction because point mutation of a nearby conserved residue has broader effects. Specifically, mutation of the aromatic residue Phe-1395 not only altered the ability of nNOS to discriminate between NADPH and NADH but also relieved the repression of electron transfer and catalysis that is normally observed in the CaM-free state (59). Thus, although Asp-1393 and Phe-1395 lie just upstream in sequence from the CaM-responsive C-terminal regulatory element in nNOS (Fig. 1) (14, 60), our data suggest that Asp-1393 is less involved in regulation compared with Phe-1395. In general, the extensive integration of conserved and unique structural elements in the NOS flavoprotein (20, 59–64) makes it difficult to predict experimental outcomes but also promises to provide new perspectives on flavoprotein function and regulation.

Acknowledgments—We thank members of the Getzoff and Tainer laboratories for helpful discussion.

REFERENCES

1. Bishop, C. D., and Brandhorst, B. P. (2003) *Evol. Dev.* **5,** 542–550
2. Brown, G. C., and Bal-Price, A. (2003) *Mol. Neurobiol.* **27,** 325–355
3. Ignarro, L. J. (ed) (2000) *Nitric Oxide, Biology and Pathobiology,* Academic Press, San Diego
4. Marletta, M. A., Hurshman, A. R., and Rusche, K. M. (1998) *Curr. Opin. Chem. Biol.* **2,** 656–663
5. Alderton, W. K., Cooper, C. E., and Knowles, R. G. (2001) *Biochem. J.* **357,** 593–615
6. Daff, S., Noble, M. A., Rivers, S. L., Chapman, S. K., Munro, A. W., Fujiwara, S., Rozhkova, E., Sagami, I., and Shimizu, T. (2001) *Biochem. Soc. Trans.* **29,** 147–152
7. Stuehr, D., Pou, S., and Rosen, G. M. (2001) *J. Biol. Chem.* **276,** 14533–14536
8. Nishida, C. R., Knudsen, G., Straub, W., and Ortiz de Montellano, P. R. (2002) *Drug Metab. Rev.* **34,** 479–501
9. Wei, C. C., Crane, B. R., and Stuehr, D. J. (2003) *Chem. Rev.* **103,** 2365–2383
10. Gorren, A. C., and Mayer, B. (2002) *Curr. Drug Metab.* **3,** 133–157
11. Miller, R. T., Martasek, P., Omura, T., and Masters, B. S. S. (1999) *Biochem. Biophys. Res. Commun.* **265,** 184–188
12. Abu-Soud, H. M., Ichimori, K., Nakazawa, H., and Stuehr, D. J. (2001) *Biochemistry* **40,** 6876–6881
13. Abu-Soud, H. M., Ichimori, K., Presta, A., and Stuehr, D. J. (2000) *J. Biol. Chem.* **275,** 17349–17357
14. Roman, L. J., Martasek, P., Miller, R. T., Harris, D. E., de La Garza, M. A., Shea, T. M., Kim, J. J., and Masters, B. S. (2000) *J. Biol. Chem.* **275,** 29225–29232
15. Guan, Z. W., and Iyanagi, T. (2003) *Arch. Biochem. Biophys.* **412,** 65–76
16. Adak, S., Santolini, J., Tikunova, S., Wang, Q., Johnson, J. D., and Stuehr, D. J. (2001) *J. Biol. Chem.* **276,** 1244–1252
17. Abu-Soud, H. M., and Stuehr, D. J. (1993) *Proc. Natl. Acad. Sci. U. S. A.* **90,** 10769–10772
18. Craig, D. H., Chapman, S. K., and Daff, S. (2002) *J. Biol. Chem.* **277,** 33987–33994
19. Santolini, J., Meade, A. L., and Stuehr, D. J. (2001) *J. Biol. Chem.* **276,** 48887–48898
20. Roman, L. J., Martasek, P., and Masters, B. S. (2002) *Chem. Rev.* **102,** 1179–1190
21. Wang, M., Roberts, D. L., Paschke, R., Shea, T. M., Masters, B. S., and Kim, J. J. (1997) *Proc. Natl. Acad. Sci. U. S. A.* **94,** 8411–8416
22. Gruez, A., Pignol, D., Zeghouf, M., Coves, J., Fontecave, M., Ferrer, J. L., and Fontecilla-Camps, J. C. (2000) *J. Mol. Biol.* **299,** 199–212
23. Olteanu, H., and Banerjee, R. (2001) *J. Biol. Chem.* **276,** 35558–35563
24. Finn, R. D., Basran, J., Roitel, O., Wolf, C. R., Munro, A. W., and Scrutton, N. S. (2003) *Eur. J. Biochem.* **270,** 1164–1175
25. Munro, A. W., Leys, D. G., McLean, K. J., Marshall, K. R., Ost, T. W., Daff, S., Miles, C. S., Chapman, S. K., Lysek, D. A., Moser, C. C., Page, C. C., and Dutton, P. L. (2002) *Trends Biochem. Sci.* **27,** 250–257
26. Serre, L., Vellieux, F. M., Medina, M., Gomez-Moreno, C., Fontecilla-Camps, J. C., and Frey, M. (1996) *J. Mol. Biol.* **263,** 20–39
27. Zhang, J., Martasek, P., Paschke, R., Shea, T., Masters, B. S. S., and Kim, J. J. (2001) *J. Biol. Chem.* **276,** 37506–37513
28. Karplus, P. A., Daniels, M. J., and Herriott, J. R. (1991) *Science* **251,** 60–65
29. Porter, T. D. (1991) *Trends Biochem. Sci.* **16,** 154–158
30. Lu, G., Campbell, W. H., Schneider, G., and Lindquist, Y. (1994) *Structure* **2,** 809–821
31. Bewley, M. C., Marohnic, C. C., and Barber, M. J. (2001) *Biochemistry* **40,** 13574–13582
32. Hubbard, P. A., Shen, A. L., Paschke, R., Kasper, C. B., and Kim, J. J. (2001) *J. Biol. Chem.* **276,** 29163–29170
33. Aliverti, A., Bruns, C. M., Pandini, V. E., Karplus, P. A., Vanoni, M. A., Curti, B., and Zanetti, G. (1995) *Biochemistry* **34,** 8371–8379
34. Shen, A. L., and Kasper, C. B. (1996) *Biochemistry* **35,** 9451–9459
35. Shen, A. L., Sem, D. S., and Kasper, C. B. (1999) *J. Biol. Chem.* **274,** 5391–5398
36. Aliverti, A., Deng, Z., Ravasi, D., Piubelli, L., Karplus, P. A., and Zanetti, G. (1998) *J. Biol. Chem.* **273,** 34008–34015
37. Medina, M., Martinez-Julvez, M., Hurley, J. K., Tollin, G., and Gomez-Moreno, C. (1998) *Biochemistry* **37,** 2715–2728
38. Aliverti, A., Piubelli, L., Zanetti, G., Lubberstedt, T., Herrmann, R. G., and Curti, B. (1993) *Biochemistry* **32,** 6374–6380
39. Roitel, O., Scrutton, N. G., and Munro, A. W. (2003) *Biochemistry* **42,** 10809–10821
40. Deng, Z., Aliverti, A., Zanetti, G., Arakaki, A. K., Ottado, J., Orellano, E. G., Calcaterra, N. B., Ceccarelli, E. A., Carrillo, N., and Karplus, P. A. (1999) *Nat. Struct. Biol.* **6,** 847–853
41. Senda, T., Yamada, T., Sakurai, N., Kubota, M., Nishizaki, T., Masai, E., Fukuda, M., and Mitsuidagger, Y. (2000) *J. Mol. Biol.* **304,** 397–410
42. Adak, S., Ghosh, S., Abu-Soud, H. M., and Stuehr, D. J. (1999) *J. Biol. Chem.* **274,** 22313–22320
43. Adak, S., Aulak, K. S., and Stuehr, D. J. (2001) *J. Biol. Chem.* **276,** 23246–23252

44. Abu-Soud, H. M., Feldman, P. L., Clark, P., and Stuehr, D. J. (1994) *J. Biol. Chem.* **269,** 32318–32326
45. Gachhui, R., Presta, A., Bentley, D. F., Abu-Soud, H. M., McArthur, R., Brudvig, G., Ghosh, D. K., and Stuehr, D. J. (1996) *J. Biol. Chem.* **271,** 20594–20602
46. Matsuda, H., and Iyanagi, T. (1999) *Biochim. Biophys. Acta* **1473,** 345–355
47. Boggs, S., Huang, L., and Stuehr, D. J. (1999) *Biochemistry* **39,** 2332–2339
48. Abu-Soud, H. M., Wang, J., Rousseau, D. L., Fukuto, J. M., Ignarro, L. J., and Stuehr, D. J. (1995) *J. Biol. Chem.* **270,** 22997–23006
49. Gutierrez, A., Grunau, A., Paine, M., Munro, A. W., Wolf, C. R., Roberts, G. C., and Scrutton, N. S. (2003) *Biochem. Soc. Trans.* **31,** 497–501
50. Oprian, D. D., and Coon, M. J. (1982) *J. Biol. Chem.* **257,** 8935–8944
51. Santolini, J., Adak, S., Curran, C. M., and Stuehr, D. J. (2001) *J. Biol. Chem.* **276,** 1233–1243
52. Witteveen, C. F., Giovanelli, J., Yim, M. B., Gachhui, R., Stuehr, D. J., and Kaufman, S. (1998) *Biochem. Biophys. Res. Commun.* **250,** 36–42
53. Noble, M. A., Munro, A. W., Rivers, S. L., Robledo, L., Daff, S. N., Yellowlees, L. J., Shimizu T., Sagami, I., Guillemette, J. G., and Chapman, S. K. (1999) *Biochemistry* **38,** 16413–16418
54. Gachhui, R., Abu-Soud, H. M., Ghosh, D. K., Presta, A., Blazing, M. A., Mayer, B., George, S. E., and Stuehr, D. J. (1998) *J. Biol. Chem.* **273,** 5451–5454
55. Berka, V., Chen, P. F., and Tsai, A. L. (1996) *J. Biol. Chem.* **271,** 33293–33300
56. Abu-Soud, H. M., Wang, J., Rousseau, D. L., and Stuehr, D. J. (1999) *Biochemistry* **38,** 12446–12451
57. Gorren, A. C. F., Schmidt, K., and Mayer, B. (2002) *Biochemistry* **41,** 7819–7829
58. Panda, S. P., Roman, L. J., Martasek, P., and Masters, B. S. S. (2002) *Nitric Oxide* **6,** 445
59. Adak, S., Sharma, M., Meade, A. L., and Stuehr, D. J. (2002) *Proc. Natl. Acad. Sci. U. S. A.* **99,** 13516–13521
60. Roman, L. J., Miller, R. T., de La Garza, M. A., Kim, J. J., and Siler Masters, B. S. (2000) *J. Biol. Chem.* **275,** 21914–21919
61. Knudsen, G. M., Nishida, C. R., Mooney, S. D., and Ortiz de Montellano, P. R. (2003) *J. Biol. Chem.* **278,** 31814–31824
62. Ruan, J., Xie, Q., Hutchinson, N., Cho, H., Wolfe, G. C., and Nathan, C. (1996) *J. Biol. Chem.* **271,** 22679–22686
63. Montgomery, H. J., Romanov, V., and Guillemette, J. G. (2000) *J. Biol. Chem.* **275,** 5052–5058
64. Lane, P., and Gross, S. S. (2002) *J. Biol. Chem.* **277,** 19087–19094
65. Panda, K., Adak, S., Aulak, K. S., Santolini, J., McDonald, J. F., and Stuehr, D. J. (2003) *J. Biol. Chem.* **278,** 37122–37131